UNCLASSIFIED

AD NUMBER
AD476827
LIMITATION CHANGES
TO: **Approved for public release; distribution is unlimited. Document partially illegible.**
FROM: **Distribution authorized to U.S. Gov't. agencies and their contractors; Critical Technology; JAN 1966. Other requests shall be referred to Directorate of Armament Development, Eglin AFB, FL. Document partially illegible. This document contains export-controlled technical data.**
AUTHORITY
AEDC ltr, 28 Mar 1975

THIS PAGE IS UNCLASSIFIED

AEDC-TR-65-258

FREE-FLIGHT RANGE TESTS OF THE 20-MM M56A2 SHELL WITH THE M505E3 FUZE

G. L. Winchenbach, R. M. Watt, and C. J. Welsh

ARO, Inc.

January 1966

~~This document is subject to special export controls and each transmittal to foreign governments or foreign nationals may be made only with prior approval of Directorate of Armament Development, Eglin AFB.~~

VON KÁRMÁN GAS DYNAMICS FACILITY
ARNOLD ENGINEERING DEVELOPMENT CENTER
AIR FORCE SYSTEMS COMMAND
ARNOLD AIR FORCE STATION, TENNESSEE

NOTICES

FREE-FLIGHT RANGE TESTS OF THE 20-MM M56A2 SHELL WITH THE M505E3 FUZE

G. L. Winchenbach, R. M. Watt, and C. J. Welsh
ARO, Inc.

FOREWORD

The work reported herein was done at the request of the Air Force Research and Technology Division (RTD), Air Force Systems Command (AFSC), Eglin Air Force Base, Florida, under Program Element 63406124, System 670A.

The results of tests presented were obtained by ARO, Inc. (a subsidiary of Sverdrup and Parcel, Inc.), contract operator of the Arnold Engineering Development Center (AEDC), AFSC, Arnold Air Force Station, Tennessee, under Contract AF 40(600)-1200. The tests were conducted during the period from April 20 to August 13, 1965, under ARO Project No. VG0554, and the manuscript was submitted for publication on November 10, 1965.

The authors wish to acknowledge the contribution of R. E. Knapp in the launching of the 20-mm rounds during the test program.

This technical report has been reviewed and is approved.

Darreld K. Calkins
Major, USAF
AF Representative, VKF
DCS/Test

Jean A. Jack
Colonel, USAF
DCS/Test

ABSTRACT

Results of free-flight range tests of the 20-mm M56A2-M505E3 shell over a Mach number range from 1.24 to 4.67 and at simulated altitudes up to 60,000 ft are presented. Measurements indicate that the arming ball rotor of the M505E3 fuze can have a pronounced adverse effect on the damping characteristics of the shell, with the severity becoming greater with increasing altitude.

CONTENTS

ILLUSTRATIONS

TABLES

NOMENCLATURE

C	Constant in Eq. (1)
C_D	Drag coefficient for nonzero yaw angle
C_{D_o}	Drag coefficient for zero yaw angle
C_{M_α}	Static-stability derivative
$C_{M_{p\alpha}}$	Magnus-moment derivative
$C_{M_q} + C_{M_{\dot{\alpha}}}$	Damping-in-pitch derivatives, $\frac{\partial C_M}{\partial q(d/V)} + \frac{\partial C_M}{\partial \dot{\alpha}(d/V)}$
C_{N_α}	Normal-force derivative
cg	Position of the center of gravity, percentage of model length from the nose, see Fig. 3a
D	Damping parameter, $-C_{N_\alpha} + 2C_D + \left(\frac{d}{\sigma_y}\right)^2 \left(C_{M_q} + C_{M_{\dot{\alpha}}}\right)$
d	Model diameter, see Fig. 3a
I_x	Model moment of inertia (relative to the longitudinal axis)
I_y	Model moment of inertia (relative to a transverse axis)
i	Imaginary number
K_1, K_2, K_3	Constants in Eq. (2)
k_α^2	$I_x/(md^2)$
L	Length of range interval used in reducing stability data
ℓ	Model length, see Fig. 3a
M	Mach number, free-stream
m	Model mass
N	Number of shadowgraph stations used in reducing stability data

p	Model spin rate
p_∞	Range pressure
Re	Reynolds number based on free-stream conditions and axial length
S	Reference area based on model diameter
s	Length of range interval used in reducing drag data
V	Model velocity
x	Distance along flight path
β, α	Components of the complex yaw angle
δ^2	$\beta^2 + \alpha^2$
$\bar{\delta}^2$	$\frac{1}{s} \int_0^s \delta^2 \, ds$
μ_1, μ_2	Damping rates of vectors in Eq. (2)
ξ	Complex yaw angle, $\beta + i\alpha$
ρ	Mass density of range air
σ_y	Radius of gyration (relative to a transverse axis)
ϕ_1', ϕ_2'	Rates of rotation of vectors in Eq. (2)

SUPERSCRIPTS

	First derivative with respect to time
	First derivative with respect to distance

SECTION I
INTRODUCTION

A 20-mm shell currently used by the Air Force has a fuze section that contains a moving arming ball rotor. In ballistic range tests conducted several years ago at atmospheric pressure (Refs. 1 and 2), adverse effects of the moving ball on the damping characteristics of the shell were detected. In more recent range tests at Mach numbers up to about 3.0 and for simulated altitudes up to 50,000 ft (Ref. 3), somewhat larger destabilizing effects attributable to the ball fuze were indicated. A recent study made at Eglin Air Force Base indicated that the instabilities of the 20-mm shell at higher Mach numbers (around 4.0) and at high altitudes could be quite critical. Yaw angles greater than 45 deg and dispersions in the trajectory of several feet were predicted to be possible within the first 1000 ft of shell travel. The computations incorporated extrapolations of the limited aerodynamic test data of Ref. 3.

In consideration of the significance of the questionable stability of the 20-mm shell for high altitude fighter aircraft application, RTD requested in March of 1965 that tests of the 20-mm shell be conducted in the VKF 1000-ft hypervelocity range (Armament Test Cell, Hyperballistic (G)). The data required from the 1000-ft flights were velocities, yaw angles, and shell positions as functions of time or distance traveled. Although the spacing of the shadowgraph stations in Range G was selected for testing statically stable configurations (in contrast to spin-stabilized projectiles), it was felt that the desired data could be satisfactorily obtained. Later, in examining the data, it was shown that, with the exercise of particular care, the measured yawing motion of a series of the test shots could be satisfactorily "fitted" to permit obtaining stability derivatives. The derivatives, along with drag coefficients obtained, are felt to be significant and are presented in this report with the measured angular orientation and trajectory data for the shell.

Tests of the 20-mm shell were conducted over a Mach number range from 1.24 to 4.67 and over a simulated altitude range from sea level to 60,000 ft.

SECTION II
APPARATUS

2.1 RANGE

Range G consists of a 10-ft-diam, 1000-ft-long tank that is contained within an underground enclosure (see Fig. 1). It is a variable density

aerodynamic range and has an 840-ft instrumented length that includes 43 equally spaced, dual-plane shadowgraph stations. The shadowgraph system permits determining the angular orientation and position of most test configurations to within approximately ±0.25 deg and ±0.002 ft, respectively, at each station. A timing system provides corresponding timing values to within 3×10^{-7} sec. The launcher normally used with this range is a 2-stage, light-gas gun having a 2.5-in.-diam launch tube. However, this launcher was not used for the special tests reported here.

In the present tests the shells were fired from a 20-mm cannon. Two barrels, one with a rifling of one turn in 30 calibers and a second barrel with a rifling of one turn in 40 calibers, were used with the cannon which was provided by RTD. The cannon was positioned in the blast tank section of the range in contrast to the normal launcher position shown in Fig. 1. A photograph of the cannon and its support system is shown in Fig. 2, indicating that the cannon was well secured.

2.2 MODELS AND TEST CONDITIONS

Modifications made in the 20-mm shell over the past several years have resulted in several designations for the slightly different configurations. In the present tests, the shell configuration designated M56A2 with a M505E3 fuze (located in the nose section of the shell) was the primary configuration tested. A sketch of the M56A2 configuration is shown in Fig. 3a, and a shadowgram of a shell in flight is shown in Fig. 3b. The M505E3 fuze is one that contains a moving arming ball rotor. In a few rounds the ball was "fixed" with an adhesive, and a few other rounds were equipped with solid steel nose sections. These modified rounds were used to provide reference data for evaluating the effects of the moving ball fuze. Further, for comparison purposes, a few shots were fired using the T282E1 configuration with a M505A2 fuze. The M505A2 fuze also has a moving arming ball rotor and differs only slightly from the M505E3 fuze. The T282E1 configuration, used in the tests of Refs. 1 and 2, has an exterior geometry that differs slightly from the M56A2 geometry. The geometry differences are small enough, however, that no appreciable differences between the aerodynamic characteristics of the M56A2 and T282E1 configurations would be expected. The measured physical properties of the 20-mm rounds for which aerodynamic data were obtained are presented in Table I. These measurements were made at AEDC.

The initial disturbances in the yawing motion of the shells were obtained from the normal gun effects. During the program, when shell instability did not seem as great as RTD expected, there was a small effort to induce

larger initial launching disturbances. Attempts to augment the normal initial disturbances to the shells by various devices positioned at the muzzle end of the gun proved unsatisfactory. Shadowgrams and X-ray photographs were used to ensure that the rifling band was intact for all data shots.

In the present tests the range pressure was varied from atmospheric pressure down to 55 mm Hg, and the corresponding Reynolds number, based on shell length and free-stream conditions, ranged from 0.25×10^6 to 6.73×10^6.

SECTION III
DATA REDUCTION PROCEDURES

For the majority of the test shots, the drag coefficient, C_D, was evaluated by fitting a cubic equation, by the least squares method, to the time-position data. This is consistent with conventional range practices (Ref. 4). For some of the simulated high altitude shots, the deceleration of the 20-mm shell was small enough that the C_D values could be better evaluated using the slope of the curve of shell velocity as a function of distance traveled; in this procedure velocity values are computed over range intervals between consecutive shadowgraph stations. The procedure is advantageous when the velocity drop over the range interval is less than about two percent of the velocity, and, for this condition, an assumed linear velocity variation is quite satisfactory. The total drag coefficient was adjusted to a zero yaw angle with the usual relationship in range testing, viz,

$$C_D = C_{D_0} + C\,\bar{\delta}^2 \tag{1}$$

The corresponding values of C for the different test conditions were obtained from plots of C_D as a function of $\bar{\delta}^2$.

The stability derivatives were evaluated in an analysis of the angular motion of the shell with the following equation:

$$\xi = K_1 \exp\left[(\mu_1 + i\phi_1')x\right] - K_2 \exp\left[(\mu_2 + i\phi_2')x\right] + K_3 \exp(ipx) \tag{2}$$

Equation (2), defining tricyclic motion, is the solution of the linear differential equation (Ref. 5) for general rolling, yawing model motion. Its use is restricted to models having slight configurational asymmetries, linear variations of force and moment with yaw angle, and a constant p/V ratio. Equation (2) is fitted to the variations of the measured components of the complex yaw angle with distance traveled, using a differential corrections procedure. There are ten equation constants to be determined in fitting Eq. (2). The K's, in general, are complex numbers; however,

p can be expressed as a function of ϕ_1' and ϕ_2'. The desired stability parameters can be expressed in terms of the determined equation constants by the following relationships:

$$C_{M_\alpha} = (2I_y/d\rho s)\ \phi_1'\phi_2' \tag{3}$$

$$D = (\mu_1 + \mu_2)(2m/\rho s) \tag{4}$$

$$C_{M_{p\alpha}} = \left[T(2m/\rho s) - C_{N_\alpha} + C_D\right] k_\alpha^2 \tag{5}$$

where

$$T = 1/2\left\{\left[(\mu_1 - \mu_2)(\phi_1' - \phi_2')\Big/(\phi_1' + \phi_2')\right] - (\mu_1 + \mu_2)\right\} \tag{6}$$

In fitting an equation using the differential corrections procedure, which is an iterative process, it is necessary to determine first a set of approximate or initial values for the equation constants to be evaluated. The errors in the determined initial values must be sufficiently small to permit the iterative process to converge. In determining the initial values for a spin-stabilized shell, it is usually adequate to assign zero values for μ_1, μ_2, and K_3. The remaining initial values are normally determined from the measured angular motion as demonstrated in the sketches below.

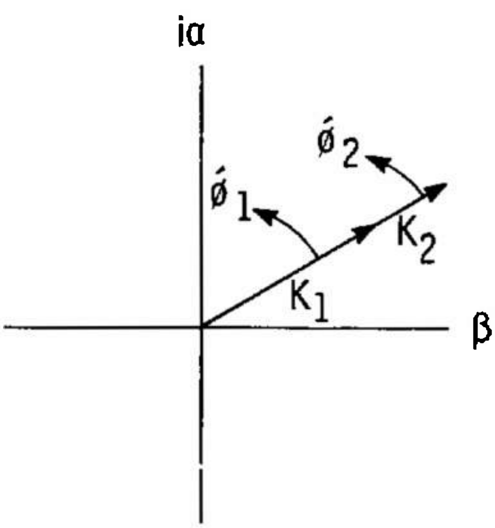

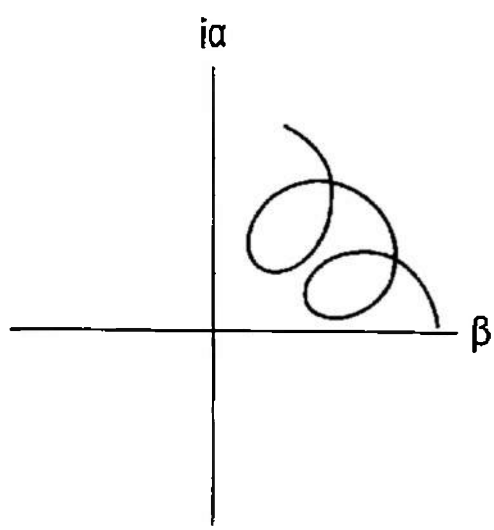

In the sketch on the left the $K_1\exp(i\phi_1'x)$ and $K_2\exp(i\phi_2'x)$ terms are shown as rotating vectors in the complex yaw plane. For a spin-stabilized shell $\phi_2' >|> \phi_1'$, and a typical pattern of the motion defined by the two vectors is shown in the sketch on the right. If the angular motion can be sufficiently defined by the plotted (β, α) values, then relationships between

the measured motion pattern and the $K_1 \exp(i\phi_1' x)$ and $K_2 \exp(i\phi_2' x)$ vectors permit obtaining adequate initial values for the ϕ_1', ϕ_2', K_1, and K_2 parameters.

To give an indication of a typical motion pattern, the 20-mm shell at M = 3.5 and atmospheric pressure has a shell travel distance per loop of the motion pattern of approximately 17.5 ft. In a ballistic range designed for testing spin-stabilized projectiles, the station spacing is usually about 5 ft or less in portions of the range; hence, the basic motion pattern usually can be defined adequately with the measured (β, α) values. In Range G with a nominal station spacing of 20 ft (on the order of one station per loop) the problem of defining the motion pattern of a spin-stabilized shell can be critical. The problem has been magnified in the present tests because of the wide bands of range pressure and Mach number of the tests in conjunction with using different barrel rifling. To circumvent this problem, initial values for the ϕ''s were evaluated from a simplified equation of motion, i.e.,

$$\xi'' - i(p/V)(I_x/I_y)\xi' - \left(\rho s d C_{M_\alpha}/2I_y\right)\xi = 0 \tag{7}$$

where

$$\phi'\text{'s} = (I_x/2I_y)(p/V) \pm \sqrt{\left[(I_x/2I_y)(p/V)\right]^2 - \left(\rho s d C_{M_\alpha}/2I_y\right)} \tag{8}$$

Equation (7) defines the model motion corresponding to conditions for $C_{N_\alpha} = (C_{M_q} + C_{M_{\dot\alpha}}) = 0$; however, it furnishes excellent approximations for the angular velocities of the two rotating vectors of an axisymmetric model having nonzero values for the C_{N_α} and $(C_{M_q} + C_{M_{\dot\alpha}})$ derivatives. In evaluating ϕ''s for a test shot with Eq. (8), the p/V ratio was determined from the nominal rifling of the barrel, and an approximate C_{M_α} value was obtained from available experimental data. By using the ϕ's evaluated by the above procedure, the corresponding initial values for the components of the amplitudes of the two vectors were approximated from the plotted (β, α) values. This approach proved extremely useful as the quality of the initial values for the ϕ''s is, in general, particularly sensitive in the curve fitting procedure.

The angular motion of several test shots was too small to permit a stability analysis. However, it should be pointed out that some test shots with motion of sufficient amplitude required more than one attempt to determine an adequate set of initial values for the amplitudes of the two vectors; further, there were a few shots, with sufficient amplitude but having critical motion patterns, for which a satisfactory set of initial values could not be found.

SECTION IV
RESULTS AND DISCUSSION

Results of the present tests of the 20-mm shell are tabulated in Table II. The various aerodynamic parameters obtained are presented in Figs. 4 through 10. Also shown in some of the figures for comparison purposes are data for the 20-mm shell from Refs. 1 and 3. All test shots of modified rounds are defined in Table I. However, for simplicity the aerodynamic data presented in the figures for modified rounds incorporating steel noses are included in the category of "ball-fixed" data.

It is significant in view of the previously mentioned analytical study that the experimental data of Table II indicate rather small values for the maximum amplitude of the yawing motion and for the dispersion in the trajectory data. The maximum amplitude of the yawing motion measured in the 1000-ft range tests was about 17 deg. The maximum angular motion measured corresponded to rounds with fuzes having arming ball rotors. No apparent correlation of the amplitude of the angular motion with altitude was indicated. It was difficult to evaluate shell dispersion because it was necessary to adjust the barrel alignment during the tests to compensate for gravity effects when the launch velocity was changed. However, the downrange positions of the many rounds relative to the nominal centerline of the range indicate that there were no appreciable altitude effects or fuze effects in the dispersion of the rounds over the range length for the tests reported herein.

Drag coefficient as a function of Mach number is shown in Fig. 4a. The figure includes data points measured at the various simulated altitudes and some from Ref. 3. Although the drag coefficient is listed in Fig. 4a as C_{D_o}, the plot includes some C_D values corresponding to small amplitude shots for which $\bar{\delta}^2$ values were not evaluated. However, for the restricted shell amplitudes the differences between C_D and C_{D_o} values are not appreciable. The C_{D_o} values of the present tests do not indicate any detectable fuze effect, and they agree well with the 20-mm shell data of Refs. 1 and 3. The apparent scatter of data in Fig. 4a is largely caused by variations in Reynolds number. The C_{D_o} values obtained at atmospheric pressure and at the 60,000-ft simulated altitude are shown in Fig. 4b to demonstrate the measured difference in the drag coefficient associated with the corresponding change in Reynolds number. In the latter figure, with the influence of Reynolds number accounted for, data scatter is slight.

The static-stability derivative, C_{M_α}, is plotted as a function of Mach number in Fig. 5. No appreciable fuze effects or altitude effects are indicated in the measurements. Data from Refs. 1 and 3 agree well with the measurements of the present tests.

The damping parameter, D, is shown in Fig. 6 as a function of Mach number. It should be noted that for a model in free flight D is more significant in defining the damping characteristics of the model than the damping-in-pitch derivatives alone. The damping values obtained in the present tests are in general agreement with data of Refs. 1 and 3 and indicate that the 20-mm shell fuze with the moving arming ball rotor can have an appreciable adverse effect on the damping characteristics of the shell. Further, the data indicate, that in general, this instability (denoted by a positive damping parameter) increased with increasing altitude. The stability analysis used in the present case presumes a rigid model; it should be pointed out that any mechanical effect from the fuze will then be measured as an apparent aerodynamic effect, and hence the measured aerodynamic parameters should be interpreted accordingly. Figure 7 presents examples of the angular motion of a round with the M505E3 fuze and of a round with the same fuze but with the ball fixed. To aid the clarity of the figure, only portions of the motions of the two rounds have been plotted. Both rounds were fired at a simulated altitude of 60,000 ft, and the measured motion clearly demonstrates the marked effect of the fuze on the damping of the shell motion at that altitude. It should be noted that the apparent inconsistencies in the measured damping values (rounds having fuzes with arming ball rotors) for similar test conditions appear quite reasonable. This follows from the known criticalness of a loose component on the damping of a simple oscillating mechanical system.

The damping-in-pitch derivatives $(C_{M_q} + C_{M_{\dot{\alpha}}})$ have been separated from the damping parameter and are presented in Fig. 8. Variations in the $(C_{M_q} + C_{M_{\dot{\alpha}}})$ values with Mach number are similar to the variations in the total damping measurements. In separating the $(C_{M_q} + C_{M_{\dot{\alpha}}})$ values from the total damping parameter, C_{N_α} values from Ref. 1 were used.

The Magnus-moment derivative, $C_{M_{p\alpha}}$, as a function of Mach number is shown in Fig. 9. The measurements are in general agreement with the data from Refs. 1 and 3, and no detectable fuze effects are indicated.

The damping rates of the precessional and nutational vectors are shown as functions of Mach number in Fig. 10 for the simulated altitude of 60,000 ft. The measurements indicate that the damping effect attributable to the shell fuze (with the arming ball rotor) is primarily restricted to the nutational vector. This is consistent with the measurements at atmospheric pressure reported in Ref. 1.

There were no detectable amplitude or rifling effects indicated in any of the data obtained for the ranges of these two parameters covered in the

tests. It should be noted that the motion of a shell can be affected by the initial conditions. However, the cannon that was used in the present tests was particularly well secured, as previously discussed. Consistent with previous comments, there were certain combinations of test conditions for which it was difficult to obtain stability data (see Table II). For example, in tests at atmospheric pressure the change in p/V over the length of the range was too large to permit fitting the yaw equation to the measured motion. However, the motion could be fitted over portions of the range. Another set of critical test conditions was at the simulated altitude of 60,000 ft and a barrel rifling of one turn in 40 calibers. For these conditions the shell traveled approximately 20 ft longitudinally per loop of the angular motion pattern. Hence, the angular values of the motion (in the complex yaw plane) measured at the shadowgraph stations tended to be grouped together. Although the combination of critical test conditions and small amplitude motion has limited the amount of stability data obtainable from the present tests, the data obtained should be very useful in an analysis of the 20-mm M56A2 shell configuration.

SECTION V
CONCLUDING REMARKS

Results of tests conducted in Range G indicate that the 20-mm M56A2 rounds had much smaller dispersion and angular motion than predicted in a previous analytical study made at Eglin Air Force Base. The arming ball rotor of the M505E3 fuze produced a marked degree of dynamic instability at the simulated 60,000-ft altitude in the present tests. A smaller drag coefficient was measured throughout the Mach number range at the 60,000-ft simulated altitude than was measured at atmospheric pressure. Static stability, Magnus moment, and drag coefficients at lower simulated altitudes and Mach numbers are in good agreement with previously published results.

REFERENCES

1. Boyer, Eugene D. "Aerodynamic Characteristics for Small Yaws of 20 mm Shell, HEI, T282E1 with Fuze M505 for Mach Numbers .36 to 3.78." BRL-MR-916, August 1955.

2. Boyer, Eugene D. "Comparison of Aerodynamic Characteristics of 20 mm, HEI, T282E1 Shell with Fuze M505 and 20 mm, HEI, T282E1 Shell with Fuze T321." BRL-TN-1055, December 1955.

3. Oliphint, J. B. "Investigation of the Ballistics of 20 mm M-56 Ammunition." Military Physics Research Laboratory, University of Texas, MPRL 569, 15 July 1964.

4. Murphy, C. H. "Data Reduction for the Free Flight Spark Ranges." BRL-R-900, February 1954.

5. Murphy, C. H. "Advances in the Dynamic Analysis of Range Data." BRL-MR-1270, May 1960.

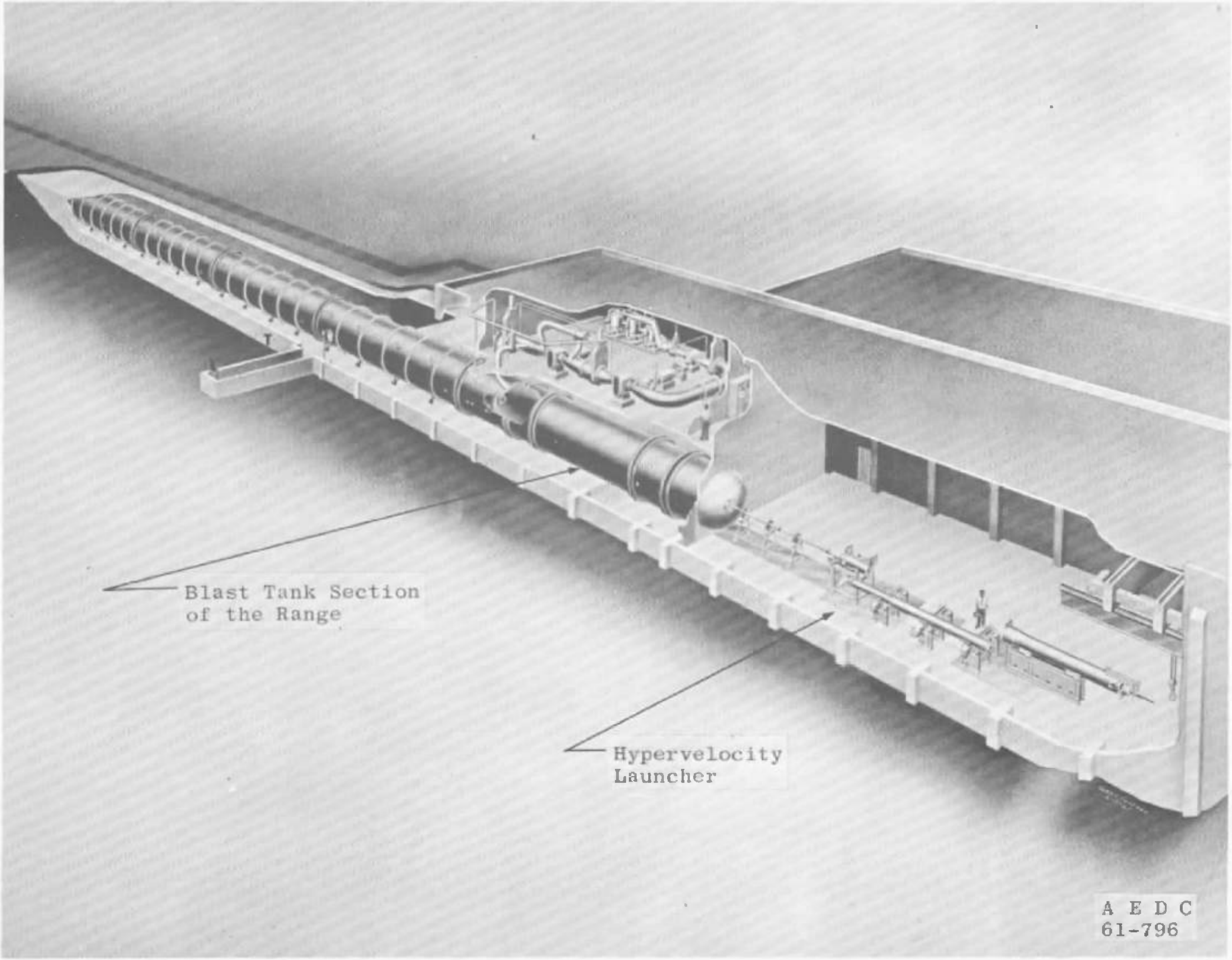
Blast Tank Section
of the Range
Hypervelocity
Launcher
A E D C
61-796

Fig. 1 Range G

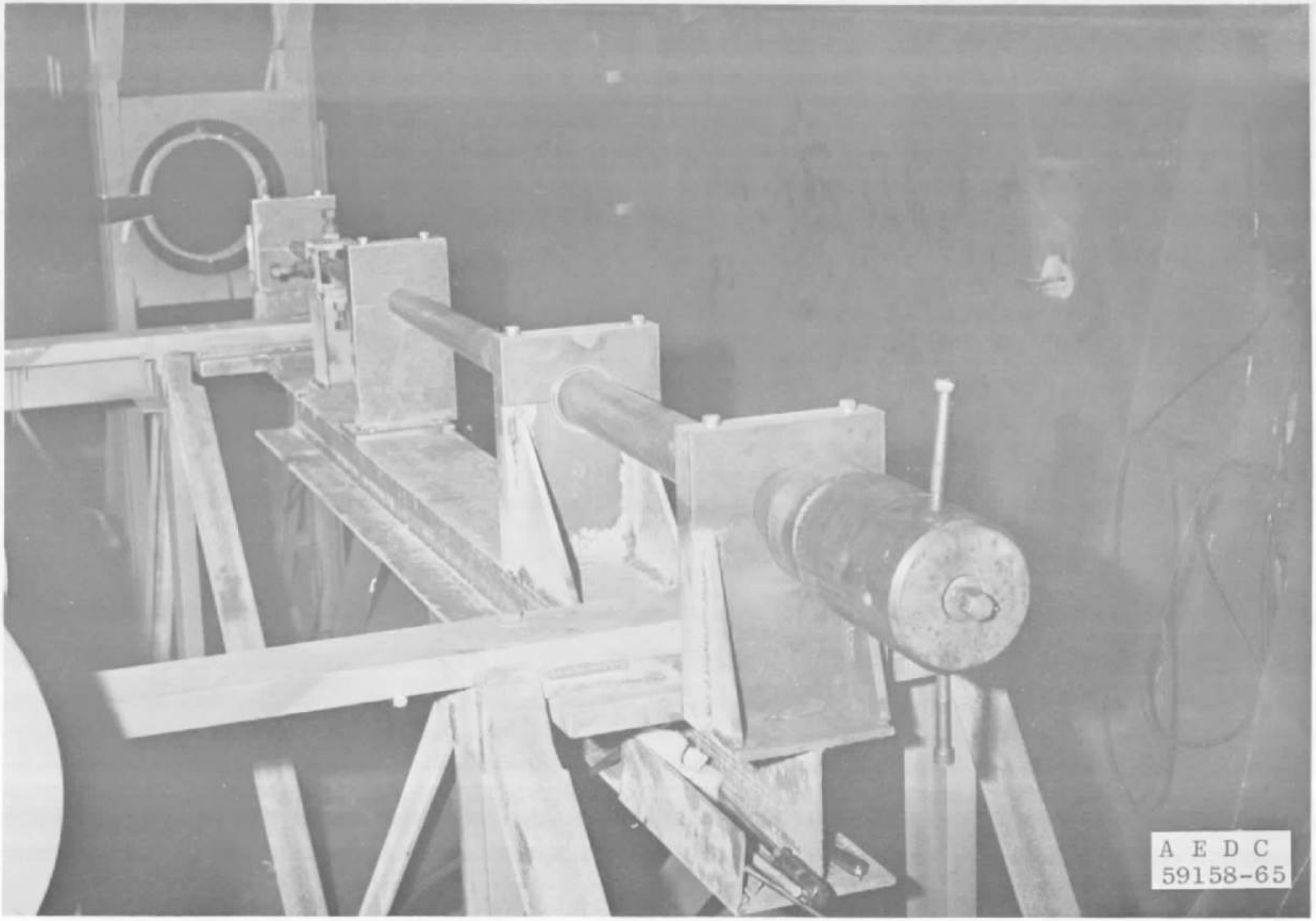

Fig. 2 Support System for the 20-mm Cannon

M56A2 - M505E3

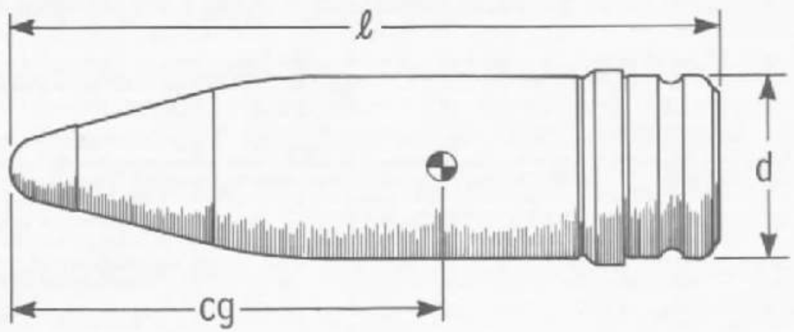

See Table I for Values of ℓ, d, and cg for Individual Rounds

a. Sketch of the Shell

Fig. 3 The 20-mm Shell

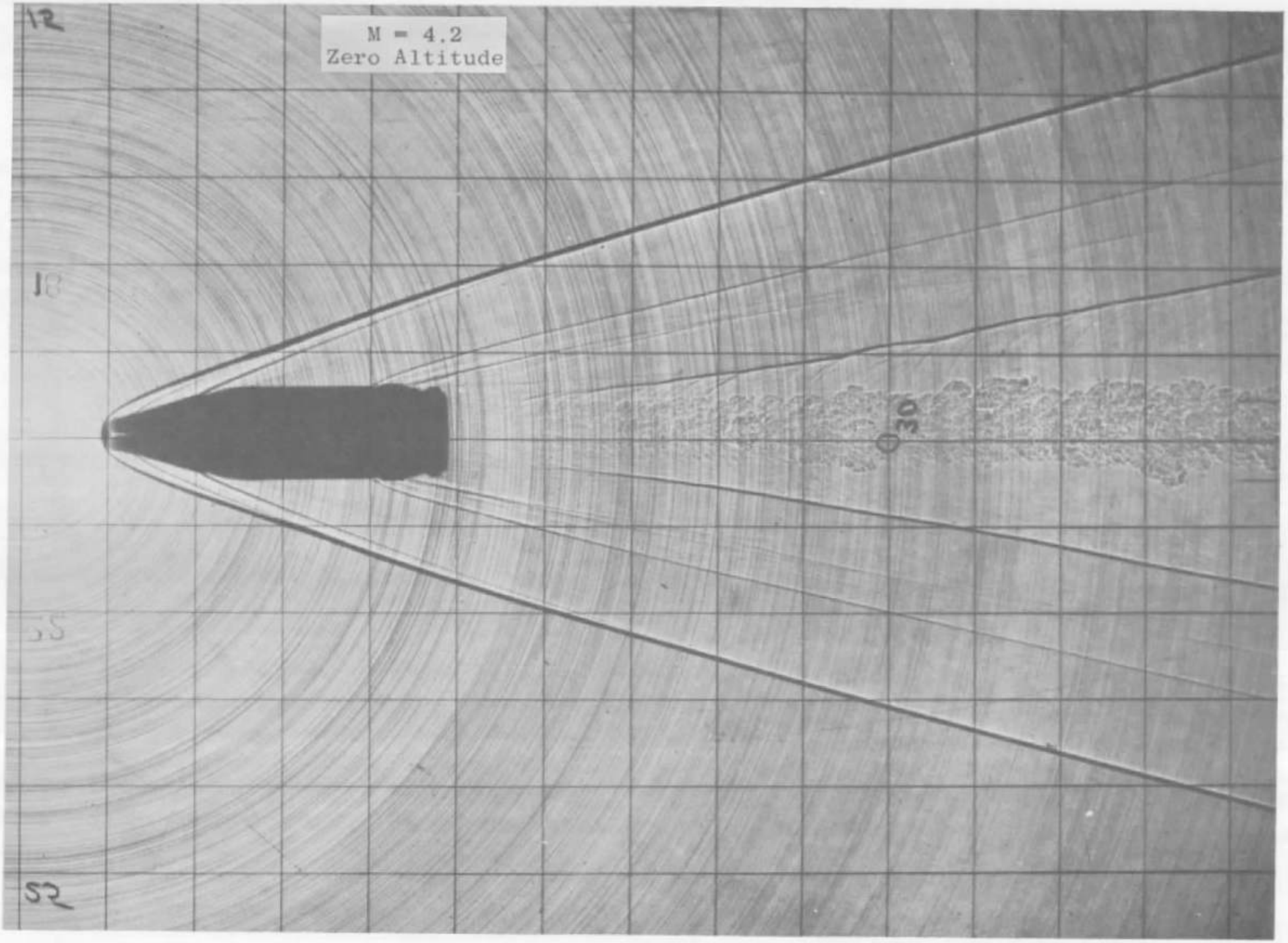

b. A Shadowgram of the Shell in Free Flight

Fig. 3 Concluded

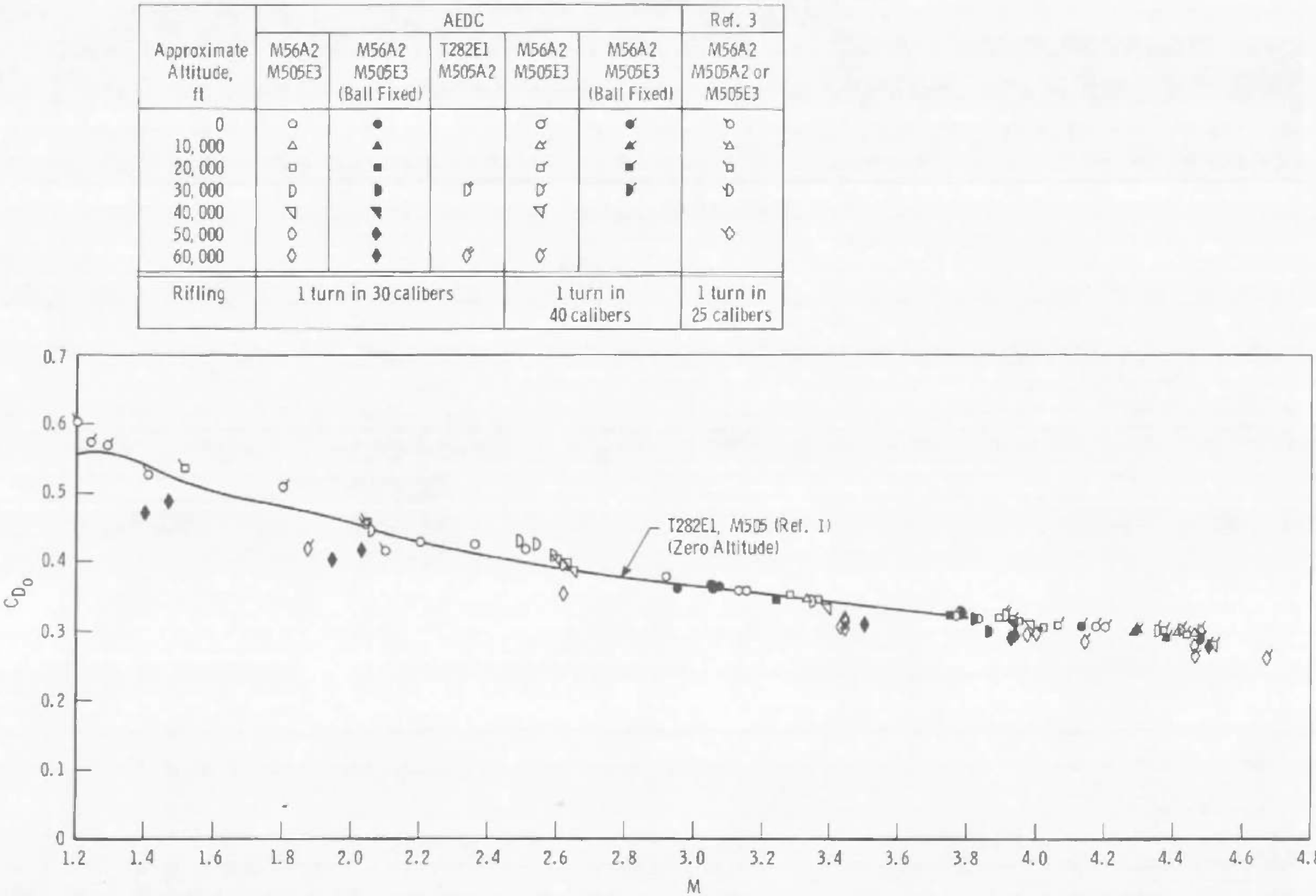

a. Data for Simulated Altitudes up to 60,000 ft (with Corresponding Variation of Reynolds Number)

Fig. 4 Drag Coefficient for Zero Yaw Angle

Approximate Altitude, ft	M56A2 M505E3	M56A2 M505E3 (Ball Fixed)	T282E1 M505A2	M56A2 M505E3	M56A2 M505E3 (Ball Fixed)
0	○	●		○́	●́
60, 000	◊	♦	◊́	◊́	♦́
Rifling	1 turn in 30 calibers			1 turn in 40 calibers	

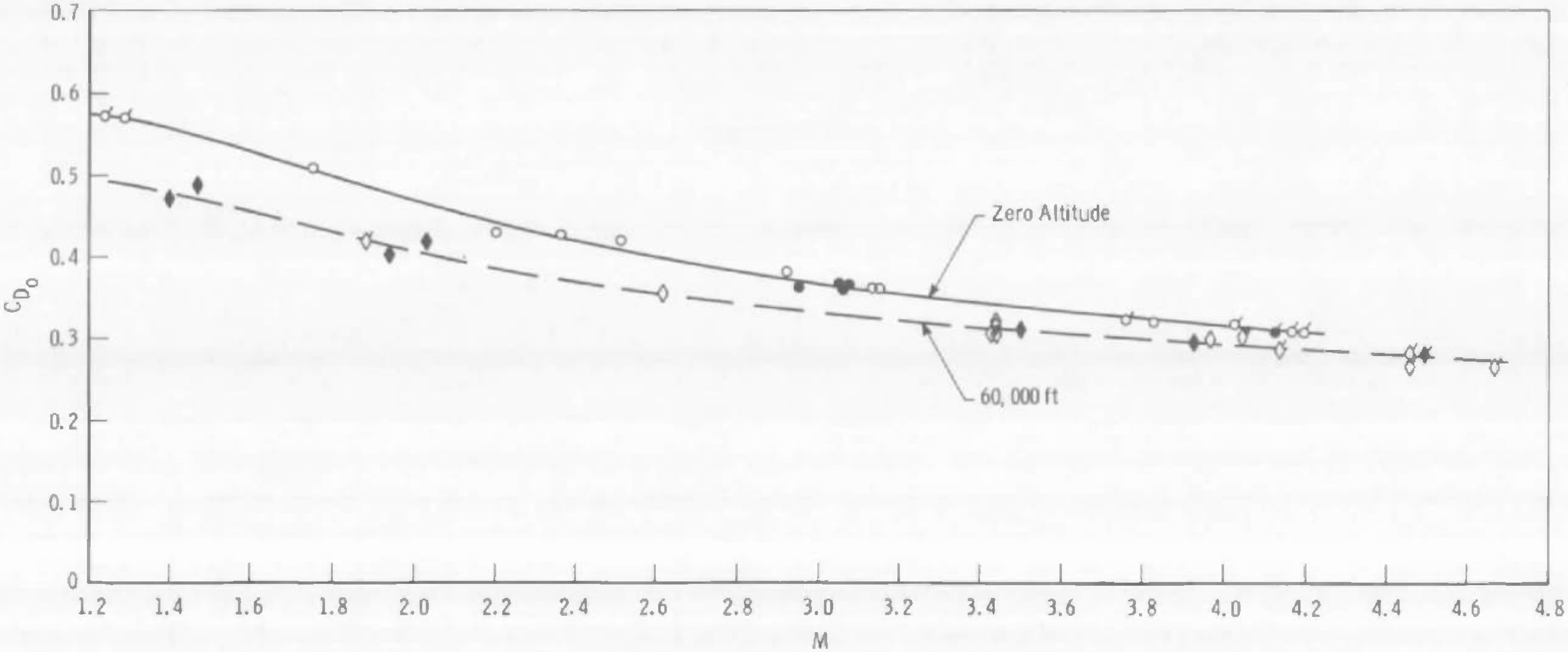

b. Data for Simulated Altitudes of 0 and 60,000 ft (AEDC)

Fig. 4 Concluded

Approximate Altitude, ft	AEDC M56A2 M505E3	AEDC M56A2 M505E3 (Ball Fixed)	AEDC T282E1 M505A2	AEDC M56A2 M505E3	AEDC M56A2 M505E3 (Ball Fixed)	Ref. 3 M56A2 M505A2 or M505E3
0	○	●		○		○
10, 000				△		△
20, 000	□	■		□		□
30, 000	▷	▶		▷	▶	▷
40, 000	◁	◀				
50, 000	◇	◆				◇
60, 000	◇	◆	◇			
Rifling	1 turn in 30 calibers			1 turn in 40 calibers		1 turn in 25 calibers

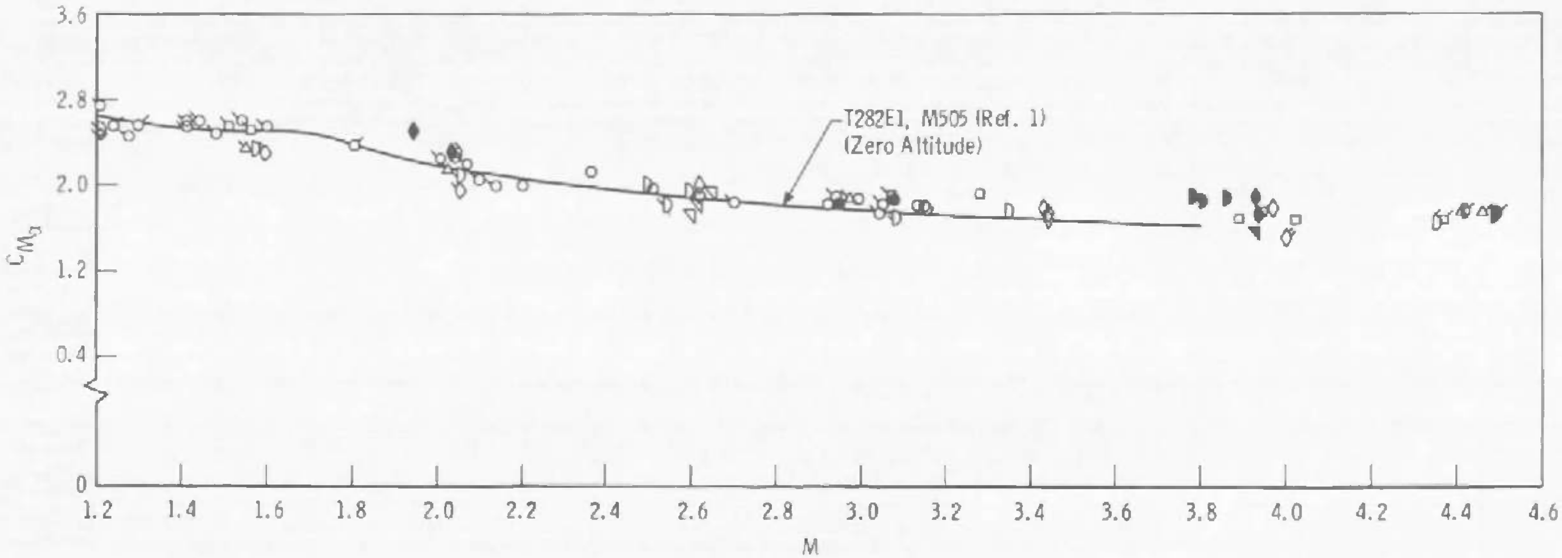

Fig. 5 Static-Stability Derivative

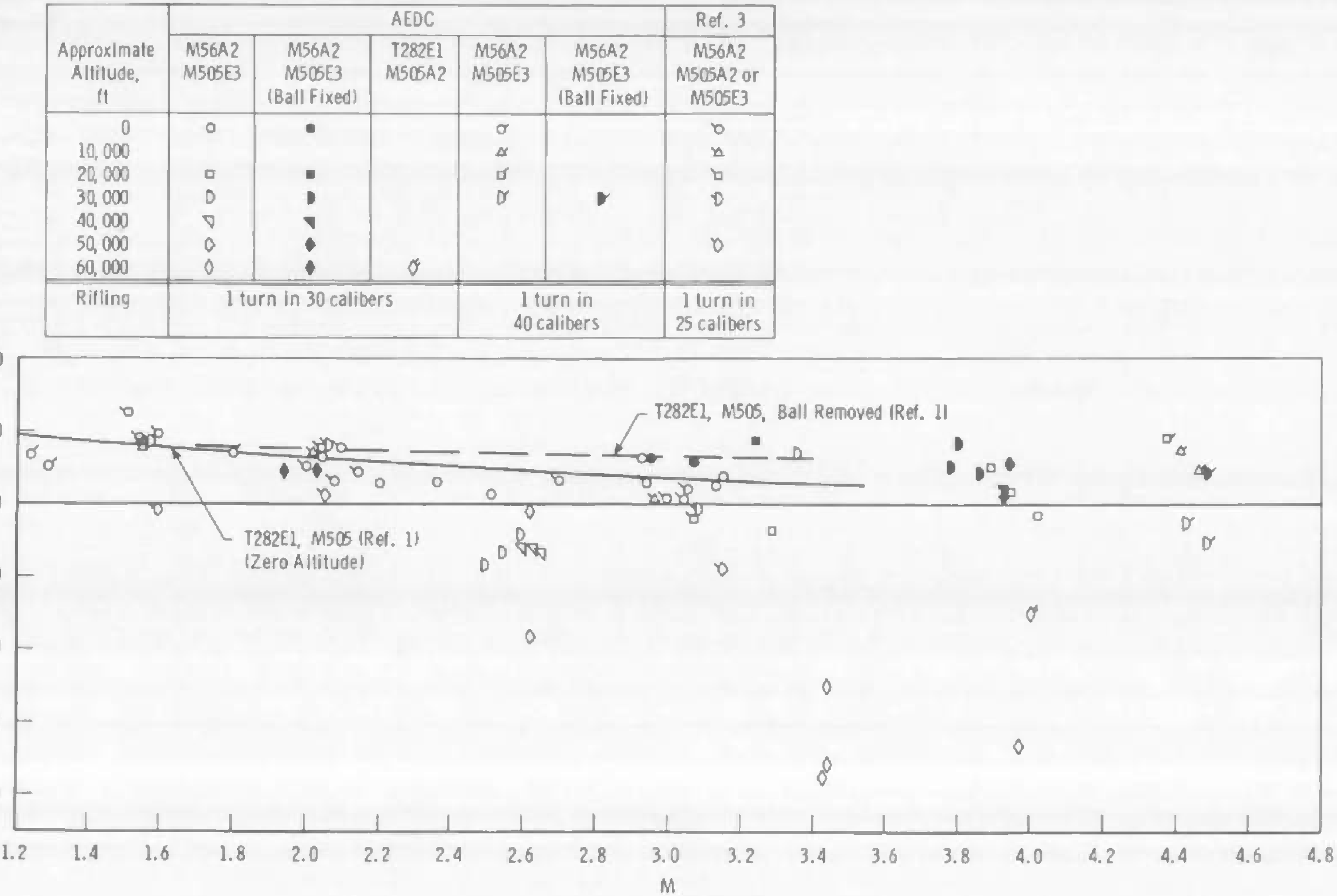

Fig. 6 Damping Parameter

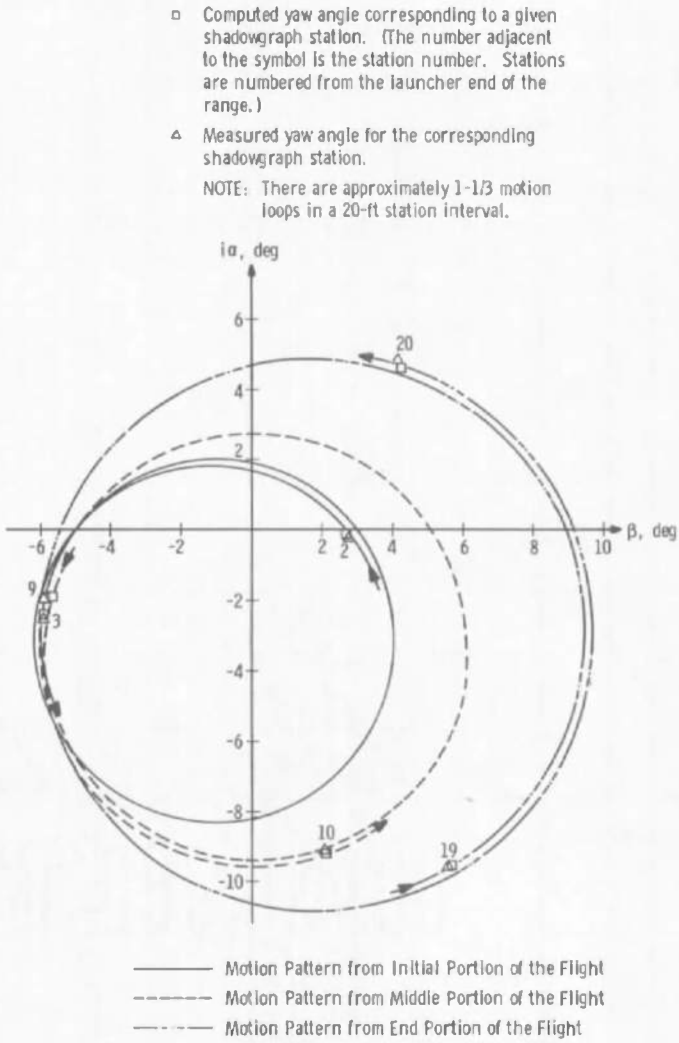

a. M = 3.97

Fig. 7 Computed Motion of the 20-mm M56A2 Shell with M505E3 Fuze at a Simulated Altitude of 60,000 ft

□ Computed yaw angle corresponding to a given shadowgraph station. (The number adjacent to the symbol is the station number. Stations are numbered from the launcher end of the range.)

△ Measured yaw angle for the corresponding shadowgraph station.

NOTE: There are approximately 1-1/3 motion loops in a 20-ft station interval.

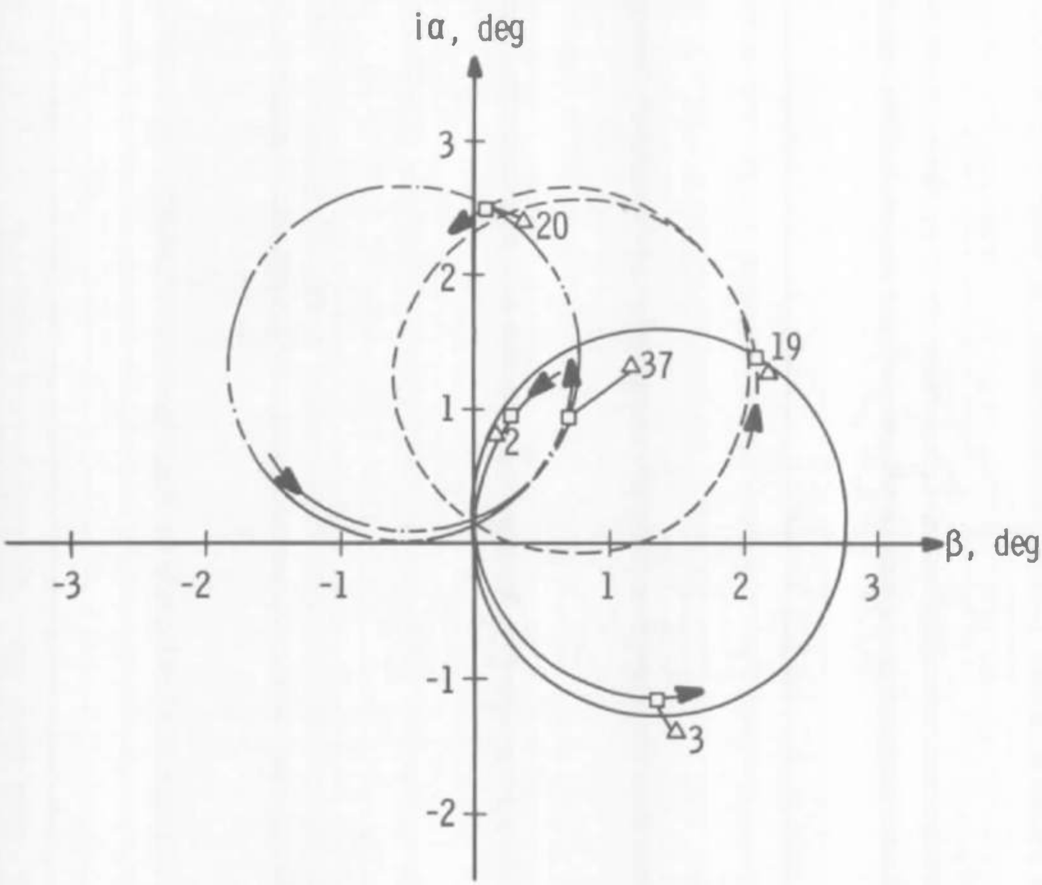

——————— Motion Pattern from Initial Portion of the Flight

- - - - - - - Motion Pattern from Middle Portion of the Flight

———-·-——— Motion Pattern from End Portion of the Flight

b. M = 3.93 (Ball Fixed)

Fig. 7 Concluded

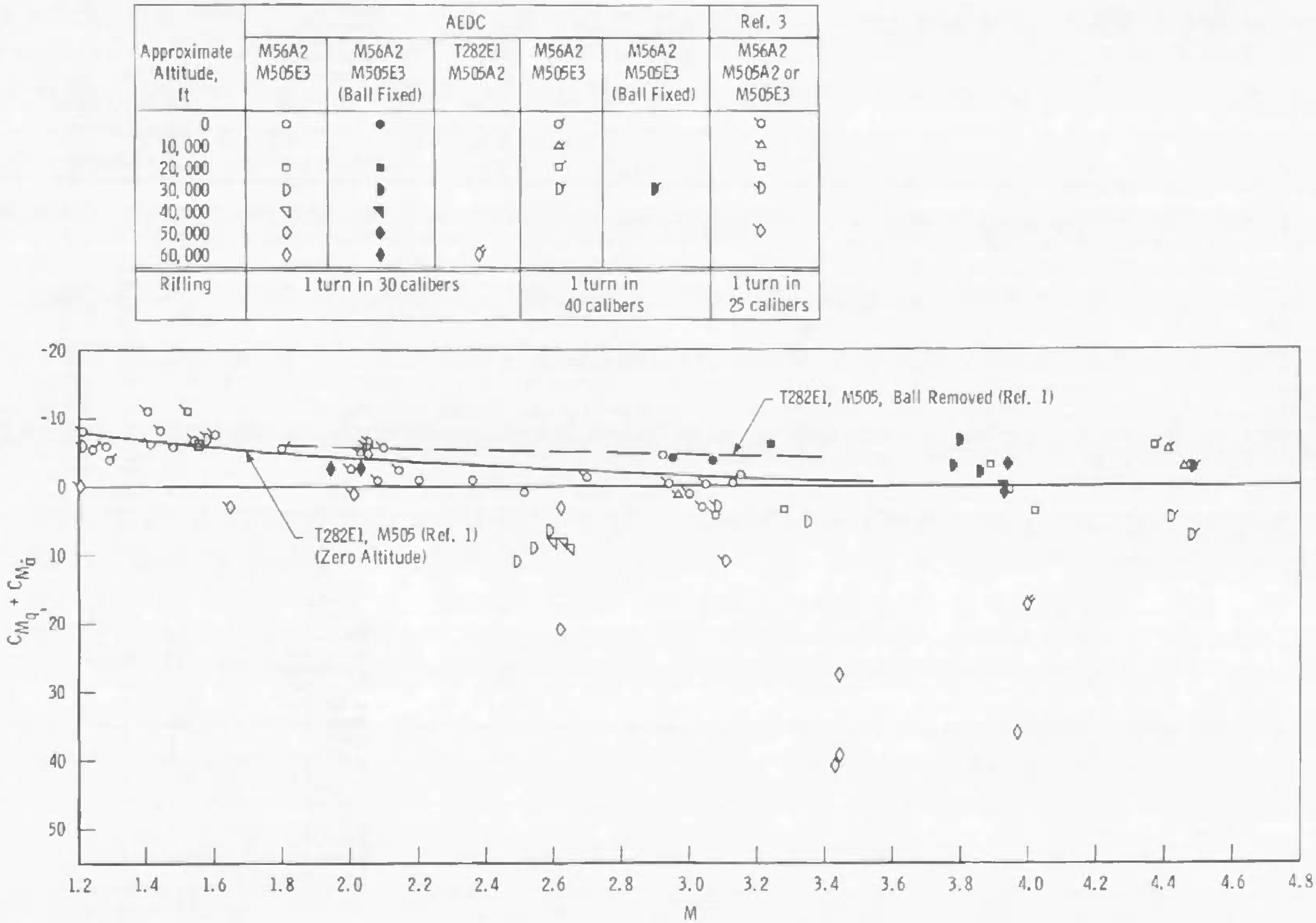

Fig. 8 Damping-in-Pitch Derivatives

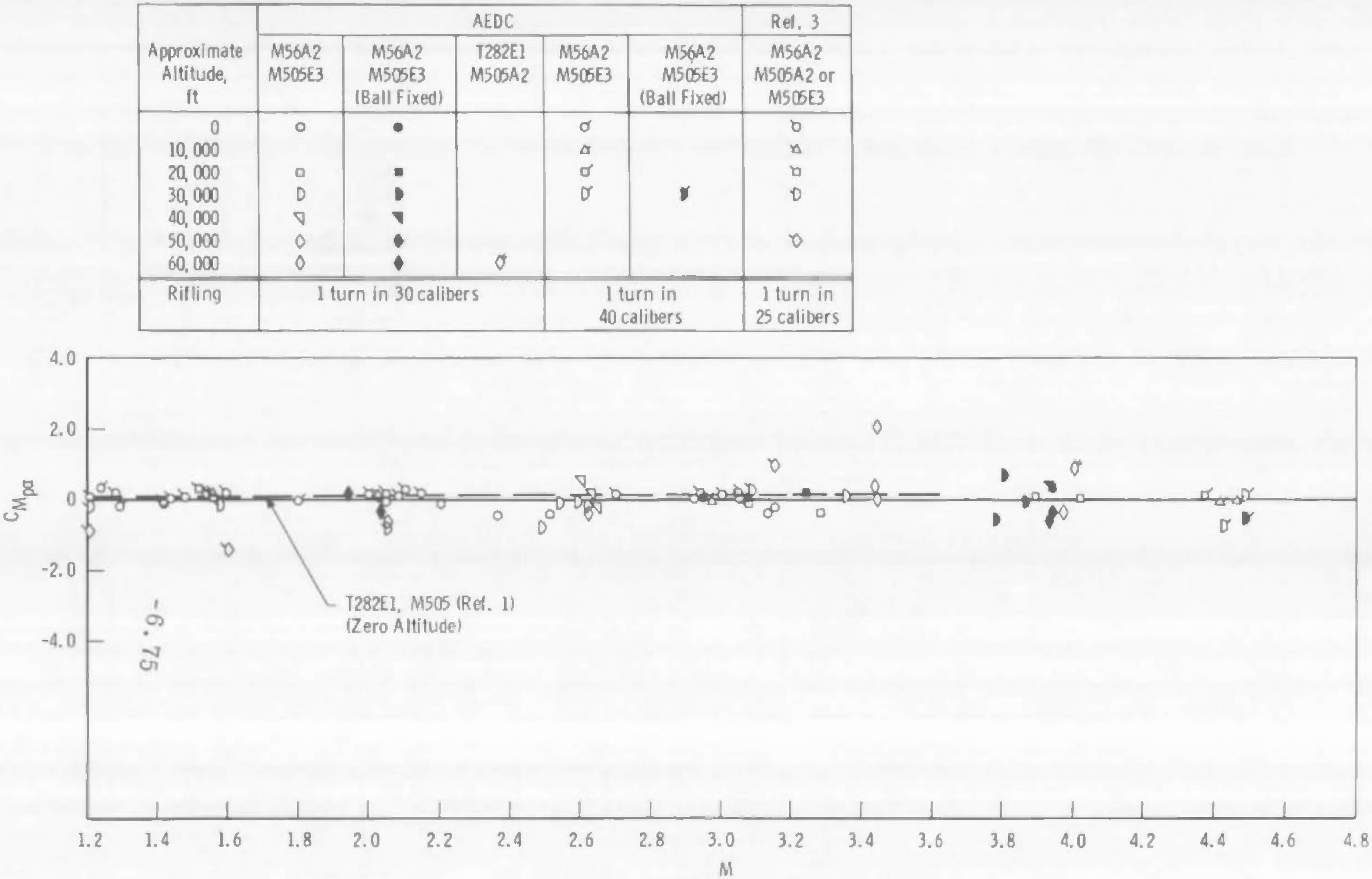

Fig. 9 Magnus-Moment Derivative

Rifling	Altitude, ft	M56A2 M505E3	M56A2 M505E3 (Ball Fixed)	T282E1 M505A2
1 Turn in 30 Calibers	60, 000	◊	♦	◊ (flagged)

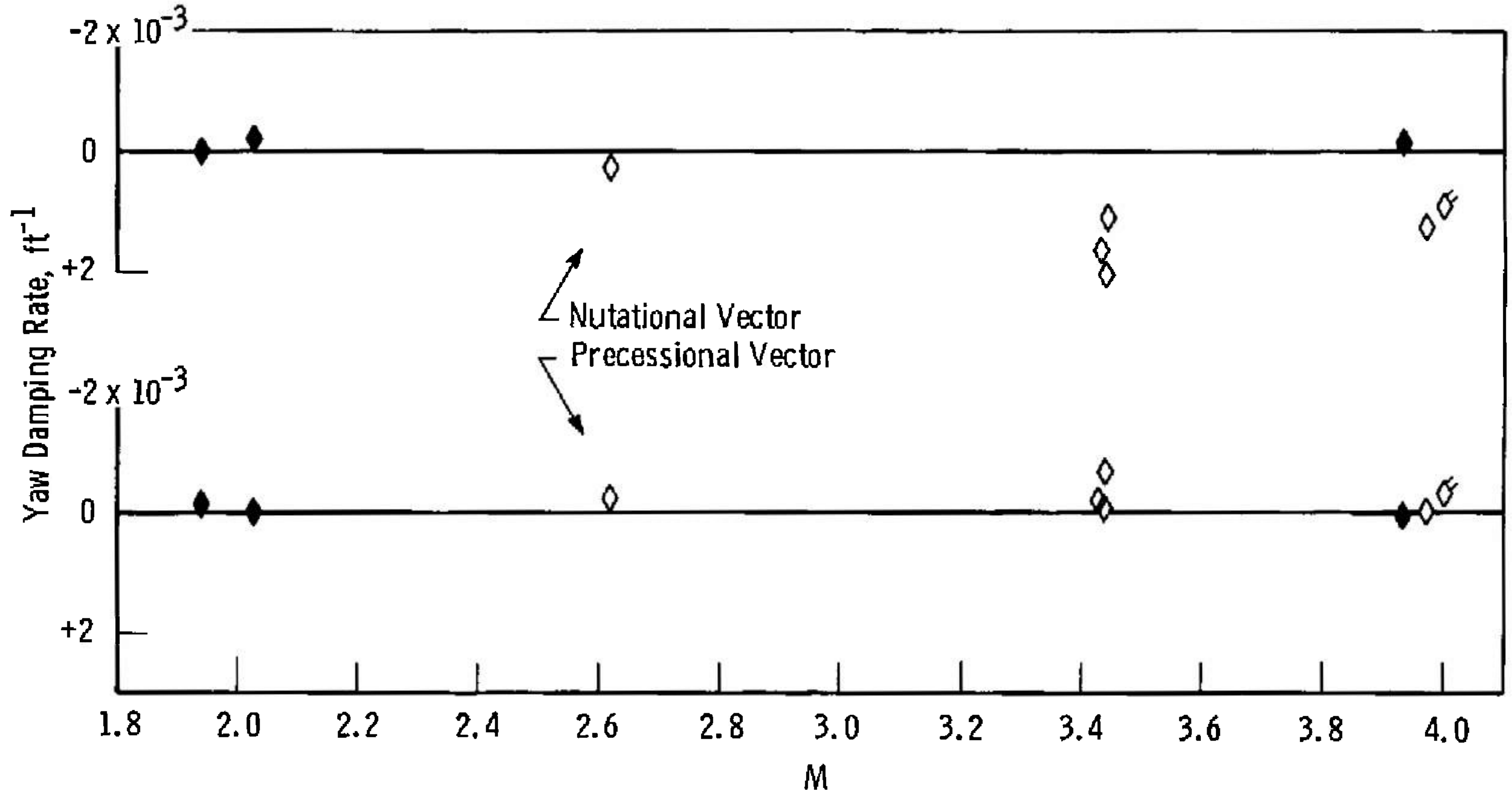

Fig. 10 Precessional and Nutational Yaw Damping Rates

TABLE I
PHYSICAL PROPERTIES OF THE 20-MM SHELL

Shot Number	Configuration	ℓ, in.	Mass, gm	cg*	$I_y \times 10^4$ in.-lb-sec^2	$I_x \times 10^4$ in.-lb-sec^2
A-1	M56A2, M505E3	2.9980	101.4440	59.31	3.694	0.4864
A-2		2.9970	101.4607	59.27	3.672	0.4867
A-3		2.9961	101.8186	59.29	3.675	0.4883
A-4		2.9922	101.9353	59.31	3.612	0.4874
A-5		3.0046	101.9696	59.43	3.706	0.4882
A-6		2.9931	101.3104	59.21	3.662	0.4860
A-7		2.9836	102.2055	59.14	3.695	0.4883
A-8		2.9950	101.4652	59.26	3.680	0.4841
A-9		2.9982	101.5321	59.19	3.678	0.4839
A-10		2.9936	101.4762	59.17	3.682	0.4865
A-11		2.9978	101.7342	59.34	3.682	0.4848
A-12		2.9928	101.7548	59.24	3.667	0.4856
A-13		2.9984	101.7775	59.28	3.709	0.4867
A-14		2.9900	101.8035	59.15	3.671	0.4821
A-15		3.0006	101.8359	59.34	3.687	0.4884
A-16		2.9977	101.9110	59.20	3.688	0.4859
A-17		2.9942	101.9123	59.16	3.680	0.4874
A-18		2.9963	101.9175	59.26	3.680	0.4876
A-19		2.9960	101.9223	59.35	3.686	0.4864
A-20		2.9985	101.9948	59.33	3.703	0.4877
A-21		2.9963	101.9952	59.40	3.688	0.4881
A-22	T282E1, M505A2	2.9838	99.8535	59.25	3.581	0.4798
A-23	M56A2, M505E3	3.0008	102.2690	59.30	3.708	0.4904
A-24		2.9950	102.2835	59.16	3.684	0.4887
A-25		2.9950	102.2665	59.22	3.692	0.4875
A-26		2.9960	102.1312	59.21	3.702	0.4906
A-27		2.9957	102.1501	59.32	3.695	0.4938
A-28	M56A2, Solid Steel Nose	2.9722	107.7655	57.24	4.024	0.4961
A-29		2.9596	107.3513	57.25	3.984	0.4974
A-30		2.9791	96.6164	56.65	3.879	0.4721
A-31		2.9711	96.5373	56.44	3.828	0.4776
A-32		2.9719	96.0071	56.36	3.818	0.4700
A-33	T282E1, M505A2	2.9846	99.7492	59.25	3.606	0.4811
A-34	T282E1, M505A2	2.9823	100.7944	59.18	3.591	0.4836
A-35		2.9828	99.5840	59.27	3.590	0.4774
A-36		2.9805	100.2305	59.24	3.599	0.4802
A-37		2.9820	99.7074	59.26	3.594	0.4798
A-38	M56A2, M505E3	2.9984	101.5244	59.01	3.660	0.4871
A-39		3.0008	101.4365	58.96	3.652	0.4960
A-40		2.9984	102.1882	59.02	3.670	0.4869
A-41		2.9999	101.1894	59.07	3.636	0.4858

TABLE I (Concluded)

Shot Number	Configuration	ℓ, in.	Mass, gm	cg*	$I_y \times 10^4$ in.-lb-sec^2	$I_x \times 10^4$ in.-lb-sec^2
A-42	M56A2, M505E3 (Ball Fixed)	2.9918	100.6556	59.12	3.618	0.4788
A-43		3.0051	101.4805	58.96	3.669	0.4847
A-44		3.0072	101.4806	58.90	3.676	0.4873
A-45		3.0042	101.2811	59.07	3.678	0.4900
A-46		3.0007	101.5422	58.96	3.661	0.4863
A-47		2.9982	101.6188	58.78	3.647	0.4852
A-48	M56A2, M505E3	3.0036	102.0689	58.83	3.663	0.4880
A-49	M56A2, M505E3 (Ball Fixed)	3.0024	102.9395	59.12	3.712	0.4964
A-50		3.0067	102.4244	58.88	3.706	0.4988
A-51		3.0098	102.2863	58.93	3.675	0.4973
A-52		3.0081	102.4363	58.94	3.710	0.4885
A-53		2.9979	102.3928	59.25	3.640	0.4904
A-54	M56A2, M505E3	3.0004	102.2744	58.98	3.674	0.4848
B-1		2.9959	102.4773	59.15	3.659	0.4884
B-2		3.0006	102.3648	59.00	3.664	0.4886
B-3		3.0016	102.2089	59.10	3.673	0.4878
B-4		3.0012	101.9575	59.10	3.663	0.4865
B-5		2.9978	102.2315	59.34	3.656	0.4909
B-6		3.0037	102.3891	58.91	3.684	0.4895
B-7		3.0015	102.3580	59.18	3.677	0.4875
B-8	M56A2, M505E3 (Ball Fixed)	2.9971	101.3611	59.38	3.651	0.4883
B-9		3.0042	102.0511	58.93	3.666	0.4869
B-10		2.9987	102.5402	59.10	3.691	0.4903
B-11		2.9996	102.5827	59.05	3.670	0.4884
B-12		2.9972	102.4038	59.07	3.672	0.5005
B-13	M56A2, M505E3	3.0024	102.1821	58.85	3.671	0.4867
B-14	M56A2, M505E3 (Ball Fixed)	2.9993	102.3513	59.17	3.684	0.4923
B-15	M56A2, M505E3	2.9979	102.4621	59.20	3.668	0.4880
B-16	M56A2, M505E3 (Ball Fixed)	3.0053	102.3822	58.94	3.705	0.4873
B-17	M56A2, M505E3	3.0032	102.4956	59.15	3.674	0.4890
B-18		3.0082	102.4064	58.91	3.695	0.4875
B-19		3.0054	102.0966	59.13	3.663	0.4917
B-20		3.0002	102.2864	58.98	3.676	0.4890
B-21		2.9920	102.3678	59.14	3.664	0.4904
B-22		3.0028	102.2375	58.93	3.674	0.4877
B-23		3.0015	102.5079	59.18	3.676	0.4908
B-24		3.0024	102.1538	59.19	3.664	0.4935
B-25		3.0011	102.5551	59.02	3.706	0.4928
B-26		2.9991	102.2230	59.26	3.670	0.4930

*Percentage of model length from the nose

NOTE: Measured model diameter (d) (for all rounds) = 0.7836 in. ±0.0013.

"A" series designates barrel rifling of one turn in 30 calibers.

"B" series designates barrel rifling of one turn in 40 calibers.

TABLE II
AERODYNAMIC PROPERTIES OF THE 20-MM SHELL

Shot Number	M	$Re \times 10^{-6}$	p_∞, mm Hg	δ^2	δ_{max}	Simulated Altitude, ft	Shell Dispersion: Distance Traveled, ft	Shell Dispersion: Horizontal Position,* in.	Shell Dispersion: Vertical Position,** in.	C_D	C_{D_0}	C_{M_α}	H	$C_{M_{p\alpha}}$	ϕ_1', deg/ft	ϕ_2', deg/ft	λ_1, ft^{-1}	λ_2, ft^{-1}	K_1, deg	K_2, deg	N	L, ft
B-1	4.20	6.73	723.0		1.7	0	923	7.27	-3.64	0.307												
B-2	4.17	6.71	723.1		1.4		943	3.48	-2.35	0.308												
B-6	4.13	6.72	731.3		2.0		923	5.87	2.70	0.308												
B-20	3.93	6.43	734.1		1.6		403	1.67	-0.36	0.317												
A-47	3.87	6.40	735.5		6.1		503	15.00	-4.34	0.340												
A-48	3.83	6.35	736.1		2.6		883	9.46	7.11	0.310												
A-15	3.83	6.34	736.3		13.4		443	5.12	-9.54	0.454												
A-17	3.82	6.30	735.1		5.2		523	-6.45	10.96	0.366												
A-16	3.81	6.29	734.4		6.6		583	-9.42	3.30	0.357												
A-33	3.79	6.23	734.0		13.0		523	-12.84	3.60	0.432												
B-21	3.76	6.14	734.1		2.7		923	3.61	-5.17	0.323												
A-22	3.65	5.65	732.9		10.0		943	-7.52	1.94	0.380												
A-6	3.15	5.24	740.8	4.6	4.0		623	7.82	11.14	0.365	0.360	1.812	-3.83	-0.207	2.017	23.81	-0.000481	-0.00180	1.31	2.26	13	320
A-1	3.13	5.13	731.3	7.2	4.5		543	-13.18	-3.54	0.369	0.360	1.815	-2.56	-0.401	2.061	22.07	0.000363	-0.00174	1.49	2.81	12	320
A-53₁	3.07	5.06	732.8	5.5	4.0		943	-6.39	8.76	0.369	0.365	1.874	-5.84	0.0602	2.152	23.00	-0.00160	-0.00150	1.96	3.09	13	280
A-53₂	2.95	4.86	732.6	3.3						0.363	0.360	1.818	-6.17	-0.0124	2.006	23.93	-0.00190	-0.00138	1.66	1.50	13	240
A-32	3.06	5.00	735.1		3.6		923	-0.63	0.34	0.362												
A-29	3.05	4.96	731.0		3.9		883	-2.66	-8.73	0.385												
A-54	2.92	4.79	731.3	3.9	4.2		943	-5.39	10.72	0.304	0.380	1.826	-6.55	0.0101	1.961	24.32	-0.00134	-0.00214	1.54	1.91	13	260
A-23₁	2.51	4.13	733.2	12.0	5.5		943	0.16	-2.87	0.429	0.420	1.979	-1.46	-0.445	2.246	23.90	0.000534	-0.00131	1.95	3.24	12	240
A-23₂	2.36	3.88	733.2	4.7						0.432	0.428	2.122	-2.99	-0.474	2.274	24.24	0.000751	-0.00235	1.30	2.17	13	260
A-23₃	2.20	3.03	733.2	1.7						0.432	0.430	2.868	-2.84	-0.148	2.088	35.78	-0.000795	-0.000774	1.05	1.00	13	260
B-26	1.60	2.06	736.9	4.3	3.6		943	-2.31	-6.41	0.613	0.508	2.381	-7.36	-0.0068	4.131	15.05	0.00131	-0.00544	1.60	1.31	12	240
B-25₁	1.29	2.12	737.2	18.0	5.1		803	0.86	-9.08	0.572	0.568	2.579	-5.25	-0.196	4.717	14.18	0.00344	0.000855	1.94	3.41	14	260
B-25₂	1.24	2.03	737.2	18.7						0.585	0.572	2.576	[illegible]	0.324	4.369	15.25	-0.000776	-0.00280	5.45	2.03	13	220
B-4	4.46	5.14	517.5	4.9	3.0	10,000	923	3.75	2.30	0.299	0.298	1.746	-4.86	-0.0097	1.940	18.45	-0.000846	-0.000893	1.48	1.74	13	280
B-3	4.41	5.11	514.4	2.9	4.9		343	1.57	1.82	0.301	0.300	1.741	-7.18	-0.0203	1.930	16.50	-0.000845	-0.00184	1.41	1.68	17	400
B-10	4.29	4.63	503.8		3.1		863	3.00	2.15	0.304												

TABLE II (Continued)

Shot Number	M	Re x 10^{-6}	P_∞, mm Hg	$\bar{\delta}^2$	δ_{max}	Simulated Altitude, ft	Shell Dispersion: Distance Traveled, ft	Shell Dispersion: Horizontal Position,* in.	Shell Dispersion: Vertical Position,** in.	C_D	C_{D_0}	C_{M_α}	D	$C_{M_{p\alpha}}$	ϕ'_1, deg/ft	ϕ'_2, deg/ft	λ_1, ft^{-1}	λ_2, ft^{-1}	K_1, deg	K_2, deg	N	L, ft
B-9	4.28	4.81	503.4		1.8	10,000	963	2.11	0.08	0.301												
A-18	[illegible]	[illegible]	400.0		4.0		[illegible]	-8.58	7.06	0.338												
A-34	[illegible]	4.38	506.0		9.5		[illegible]	1.35	11.62	0.350												
A-2	[illegible]	[illegible]	520.7		3.7		[illegible]	-8.11	-1.46	0.345												
A-7	[illegible]	4.03	341.5		4.4		923	-8.51	-6.06	0.337												
B-5	4.44	[illegible]	340.2		[illegible]	20,000	583	0.44	-0.76	0.297												
B-11	4.38	3.39	345.5		1.4		943	2.13	-1.00	0.292												
B-8	4.37	3.40	347.8	2.2	2.8		923	1.54	4.83	0.302	0.201	1.658	-8.93	0.132	1.169	17.08	-0.000785	-0.00145	1.33	1.48	28	800
B-22	4.05	3.15	345.3		1.3		[illegible]	2.86	0.60	0.310												
A-19₁	4.02	2.14	348.1	20.9	7.4		[illegible]	[illegible]	-11.74	[illegible]	[illegible]	1.830	1.57	[illegible]	0.8740	23.42	-0.000745	0.00114	2.23	3.40	13	300
A-19₂	3.94	[illegible]	[illegible]	26.5						[illegible]	[illegible]	[illegible]	[illegible]	0.316	[illegible]	[illegible]	-0.00124	0.000853	1.80	4.30	13	300
A-[illegible]	3.85	3.01	[illegible]		12.5		563	-6.67	6.87	0.424												
A-41	[illegible]	2.99	[illegible]	11.8	5.8		563	2.78	-0.35	0.335	[illegible]	1.665	-5.00	[illegible]	0.8627	[illegible]	-0.000797	[illegible]	2.06	3.18	17	400
A-42	3.75	2.90	342.5		2.8		943	2.22	[illegible]	[illegible]												
A-3	3.38	2.58	341.6		2.8		[illegible]	-1.25	2.08	0.347												
A-8	3.28	[illegible]	341.4	23.9	7.0		943	[illegible]	1.02	[illegible]	[illegible]	[illegible]	4.58	[illegible]	0.9806	23.94	-0.0000324	0.000852	1.81	4.00	13	[illegible]
A-28	[illegible]	3.42	335.8	13.5	5.0		[illegible]	3.00	11.83	0.360	0.345	[illegible]	-7.92	0.154	[illegible]	21.96	-0.000555	-0.000878	2.57	2.90	14	320
B-12	4.48	2.27	226.8	1.7	2.4	30,000	[illegible]	[illegible]	2.08	0.291	0.200	1.722	-4.29	-0.454	0.7986	17.33	0.000234	[illegible]	0.86	1.12	18	300
B-7₁	4.48	2.25	226.2	14.9	8.1		943	[illegible]	-4.40	0.315	0.302	[illegible]	5.25	[illegible]	0.7753	17.23	[illegible]	0.00147	2.31	2.81	13	280
B-7₂	4.43	2.23	226.2	20.1						0.321	0.302	1.746	2.56	-0.782	0.8032	17.42	0.000503	[illegible]	1.69	4.19	13	260
A-20	3.92	[illegible]	243.0		6.0		783	-2.22	-10.48	0.330												
A-26	[illegible]	1.04	221.0		2.6		803	-10.72	-2.94	0.326												
A-40	[illegible]	[illegible]	219.4		4.8		803	-0.53	10.45	0.335												
A-43₁	3.88	1.94	232.7	2.5	2.4		903	-0.63	-3.00	0.306	0.301	1.858	-4.33	-0.0060	0.6381	[illegible]	-0.000280	-0.000425	1.29	1.04	13	280
A-43₂	3.80	1.91	232.7	1.4						0.320	0.319	1.854	-8.39	[illegible]	[illegible]	23.86	-0.00123	-0.000139	1.22	0.89	12	300
A-43₃	3.78	1.90	232.7	1.6						0.324	0.322	[illegible]	-5.16	-0.548	0.6341	24.02	-0.000294	-0.00114	0.98	0.84	13	380
A-9	3.35	1.58	231.6	1.1	2.0		923	2.96	3.03	0.345	[illegible]	1.777	-7.23	0.0945	0.5893	23.80	-0.000522	-0.000851	0.87	0.86	31	800

TABLE II (Continued)

Shot Number	M	Re x 10^-6	p_∞, mm Hg	$\bar{\delta}^2$	δ_{max}	Simulated Altitude, ft	Shell Dispersion: Distance Traveled, ft	Shell Dispersion: Horizontal Position,* in.	Shell Dispersion: Vertical Position,** in.	C_D	C_{D_o}	C_{M_α}	D	$C_{M_{p\alpha}}$	ϕ_1', deg/ft	ϕ_2', deg/ft	λ_1, ft^{-1}	λ_2, ft^{-1}	K_1, deg	K_2, deg	N	L, ft
A-27$_1$	2.58	1.30	222.5	20.5	8.6	30,000	943	-1.30	4.02	0.433	0.410	1.843	4.10	-0.0843	0.6422	23.86	-0.000352	0.00102	2.44	3.37	13	264
A-27$_2$	2.54	1.27	222.5	29.4						0.455	0.425	1.817	6.56	-0.140	0.5918	24.19	-0.000287	0.00135	2.05	4.00	13	320
A-27$_3$	2.49	1.24	222.5	42.9						0.477	0.432	2.011	8.42	-0.805	0.6486	24.51	0.000458	0.000908	1.47	5.69	12	240
B-13	4.52	1.45	143.1		1.7	40,000	943	3.83	-2.88	0.281												
A-21	3.98	1.25	140.6		2.5		943	0.88	-0.38	0.310												
A-44	3.93	1.26	142.2	13.1	5.2		763	16.33	-6.46	0.330	0.310	1.576	-2.06	0.451	0.3344	23.87	0.000100	-0.000314	2.35	2.07	23	820
A-10	3.39	1.04	136.3		1.3		923	2.86	5.90	0.334												
A-26$_1$	2.85	0.828	136.3	20.8	8.6		943	-7.22	6.72	0.411	0.388	1.830	6.62	-0.211	0.3961	33.94	0.000120	-0.000786	2.62	3.38	13	360
A-26$_2$	2.83	0.815	138.3	27.5						0.429	0.400	1.820	5.77	0.190	0.3708	24.17	-0.000420	0.00100	2.73	3.97	14	280
A-26$_3$	2.80	0.807	138.3	34.2						0.441	0.405	1.722	5.91	0.538	0.3470	24.31	-0.000682	0.00128	2.62	4.21	14	360
B-15	4.52	0.897	88.1		5.0	50,000	783	-8.36	-9.18	0.282												
B-14	4.47	0.892	88.8		4.7		923	9.01	8.77	0.297												
A-39	3.86	0.770	86.5		5.1		523	-4.67	-9.05	0.294												
A-45	3.94	0.783	86.0	3.3	2.7		943	-2.82	-3.12	0.301	0.297	1.708	-5.65	-0.359	0.2176	23.89	0.0000148	-0.000372	1.38	1.32	30	800
A-11	3.40	0.657	88.1		9.6		943	-2.53	-7.68	0.377												
A-25	2.62	0.503	85.6	44.4	15.2		883	5.01	-11.09	0.453	0.398	1.906	18.2	-0.248	0.2405	24.05	-0.000549	-0.00188	3.18	3.91	18	440
B-18	4.07	0.584	55.8		3.7	60,000	923	3.05	3.08	0.264												
B-16	4.50	0.584	55.9	3.1	3.3		943	4.38	2.83	0.280												
B-17	4.46	0.563	58.4		3.6		923	7.45	3.80	0.265												
B-19	4.46	0.564	56.4		3.8		923	8.00	4.59	0.280												
B-23	4.14	0.514	55.4		3.0		943	3.83	3.05	0.286												
A-37	4.00	0.476	53.2	120.1	16.8		843	10.35	-10.28	0.453	0.300	1.515	15.1	0.010	0.1213	24.18	-0.000316	0.000910	5.17	7.37	19	600
A-38	3.07	0.476	53.4	52.2	17.2		883	1.89	-10.07	0.364	0.298	1.789	33.2	-0.354	0.1423	24.06	0.00000157	0.00130	3.44	4.88	14	360
A-46	3.93	0.471	53.3	3.8	3.0		863	4.45	-11.04	0.298	0.293	1.677	-1.28	-0.628	0.1492	23.95	0.0000860	-0.000135	1.35	1.43	23	700
A-31	3.50	0.418	53.5		2.6		493	-0.64	12.70	0.310												
A-30	3.45	0.407	52.9		6.0		763	-7.58	-7.63	0.315												
A-4	3.45	0.414	53.5		11.2		583	12.53	-4.85	0.375												
A-5	3.44	0.413	53.3	9.5	4.6		583	-3.61	5.17	0.316	0.302	1.737	35.7	2.06	0.1378	23.84	-0.000700	0.00209	1.19	1.67	17	440
A-12	3.44	0.414	53.8	35.8	11.0		923	1.08	-11.53	0.367	0.319	1.733	25.0	-0.0311	0.1371	24.08	-0.0000960	0.00108	2.73	3.38	34	740

TABLE II (Concluded)

Shot Number	M	Re x 10^{-6}	p_∞, mm Hg	$\bar{\delta}^2$	δ_{max}	Simulated Altitude, ft	Shell Dispersion			C_D	C_{D_o}	C_{M_α}	D	$C_{M_{p\alpha}}$	ϕ', deg/ft	ϕ'', deg/ft	μ_1, ft^{-1}	μ_2, ft^{-1}	K_1, deg	K_2, deg	N	L, ft
							Distance Traveled, ft	Horizontal Position,* in.	Vertical Position,** in.													
A-13	2.44	0.429	55.5		2.5	60,000	923	-2.16	-1.67	0.312												
A-14	3.43	0.425	55.3	75.9	15.0		843	-1.42	-10.84	0.404	0.306	1.791	37.6	0.183	0.1474	23.96	-0.000168	0.00168	2.97	4.00	37	700
A-24	2.82	0.316	52.8	5.9	4.1		943	6.58	-5.89	0.365	0.355	2.024	0.903	-0.298	0.1603	24.17	-0.000250	0.000294	1.63	1.70	36	800
A-50	2.03	0.260	55.8	11.5	5.0		943	-5.66	0.42	0.437	0.417	2.308	-4.87	-0.314	0.1877	24.14	-0.0000110	-0.000186	2.34	2.66	32	780
A-49	1.94	0.243	55.8	5.3	3.8		943	4.27	-2.06	0.410	0.403	2.505	-4.68	0.174	0.2030	24.27	-0.000155	-0.0000325	1.78	1.60	35	800
B-24	1.87	0.231	55.1		2.5		743	-8.59	2.70	0.419												
A-52	1.47	0.186	55.4		1.4		825	-2.23	-10.32	0.487												
A-51	1.40	0.175	55.7		2.3		743	3.38	-10.76	0.470												

*Positive when the shell is to the right of the range centerline.
**Positive when the shell is above the range centerline.

NOTE: Subscripts on the shot number indicate first, second, or third portion of the range length over which the listed aerodynamic data were obtained. Shell dispersion data are for the complete flight of the round. Where stability parameters are not listed, the yawing motion could not be "fitted" satisfactorily.

UNCLASSIFIED
Security Classification

DOCUMENT CONTROL DATA - R&D

(Security classification of title, body of abstract and indexing annotation must be entered when the overall report is classified)

1 ORIGINATING ACTIVITY (Corporate author) Arnold Engineering Development Center ARO, Inc., Operating Contractor Arnold Air Force Station, Tennessee	2a REPORT SECURITY CLASSIFICATION UNCLASSIFIED 2b GROUP N/A

3 REPORT TITLE

FREE-FLIGHT RANGE TESTS OF THE 20-MM M56A2 SHELL WITH THE M505E3 FUZE

4 DESCRIPTIVE NOTES (Type of report and inclusive dates)

N/A

5 AUTHOR(S) (Last name, first name, initial)

Winchenbach, G.L., Watt, R.M., and Welsh, C.J., ARO, Inc.

6 REPORT DATE	7a TOTAL NO OF PAGES	7b NO OF REFS
January 1966	38	5

8a CONTRACT OR GRANT NO AF 40(600)-1200 b. System 670 A c Program Element 63406124 d	9a ORIGINATOR'S REPORT NUMBER(S) AEDC-TR-65-258 9b OTHER REPORT NO(S) (Any other numbers that may be assigned this report) N/A

10 AVAILABILITY/LIMITATION NOTICES

~~Qualified users may obtain copies of this report from DDC. Release to foreign governments or foreign nationals must have prior approval of Research and Technology Division.~~

11. SUPPLEMENTARY NOTES N/A	12 SPONSORING MILITARY ACTIVITY Research and Technology Division Detachment 4, Air Force Systems Command, Eglin Air Force Base, Florida

13 ABSTRACT

Results of free-flight range tests of the 20-mm M56A2-M505E3 shell over a Mach number range from 1.24 to 4.67 and at simulated altitudes up to 60,000 ft are presented. Measurements indicate that the arming ball rotor of the M505E3 fuze can have a pronounced adverse effect on the damping characteristics of the shell, with the severity becoming greater with increasing altitude.

This document has been approved for public release its distribution is unlimited. Per AF Letter dtd 28 March 1975. signed William O. Cole

DD FORM 1 JAN 64 1473

UNCLASSIFIED
Security Classification

14. KEY WORDS	LINK A ROLE	LINK A WT	LINK B ROLE	LINK B WT	LINK C ROLE	LINK C WT
20-mm shell						
altitude testing						
flight characteristics						

INSTRUCTIONS

1. ORIGINATING ACTIVITY: Enter the name and address of the contractor, subcontractor, grantee, Department of Defense activity or other organization *(corporate author)* issuing the report.

2*a*. REPORT SECURITY CLASSIFICATION: Enter the overall security classification of the report. Indicate whether "Restricted Data" is included. Marking is to be in accordance with appropriate security regulations.

2*b*. GROUP: Automatic downgrading is specified in DoD Directive 5200.10 and Armed Forces Industrial Manual. Enter the group number. Also, when applicable, show that optional markings have been used for Group 3 and Group 4 as authorized.

3. REPORT TITLE: Enter the complete report title in all capital letters. Titles in all cases should be unclassified. If a meaningful title cannot be selected without classification, show title classification in all capitals in parenthesis immediately following the title.

4. DESCRIPTIVE NOTES: If appropriate, enter the type of report, e.g., interim, progress, summary, annual, or final. Give the inclusive dates when a specific reporting period is covered.

5. AUTHOR(S): Enter the name(s) of author(s) as shown on or in the report. Enter last name, first name, middle initial. If military, show rank and branch of service. The name of the principal author is an absolute minimum requirement.

6. REPORT DATE: Enter the date of the report as day, month, year; or month, year. If more than one date appears on the report, use date of publication.

7*a*. TOTAL NUMBER OF PAGES: The total page count should follow normal pagination procedures, i.e., enter the number of pages containing information.

7*b*. NUMBER OF REFERENCES: Enter the total number of references cited in the report.

8*a*. CONTRACT OR GRANT NUMBER: If appropriate, enter the applicable number of the contract or grant under which the report was written.

8*b*, 8*c*, & 8*d*. PROJECT NUMBER: Enter the appropriate military department identification, such as project number, subproject number, system numbers, task number, etc.

9*a*. ORIGINATOR'S REPORT NUMBER(S): Enter the official report number by which the document will be identified and controlled by the originating activity. This number must be unique to this report.

9*b*. OTHER REPORT NUMBER(S): If the report has been assigned any other report numbers *(either by the originator or by the sponsor)*, also enter this number(s).

10. AVAILABILITY/LIMITATION NOTICES: Enter any limitations on further dissemination of the report, other than those imposed by security classification, using standard statements such as:

(1) "Qualified requesters may obtain copies of this report from DDC."

(2) "Foreign announcement and dissemination of this report by DDC is not authorized."

(3) "U. S. Government agencies may obtain copies of this report directly from DDC. Other qualified DDC users shall request through ____________."

(4) "U. S. military agencies may obtain copies of this report directly from DDC. Other qualified users shall request through ____________."

(5) "All distribution of this report is controlled. Qualified DDC users shall request through ____________."

If the report has been furnished to the Office of Technical Services, Department of Commerce, for sale to the public, indicate this fact and enter the price, if known.

11. SUPPLEMENTARY NOTES: Use for additional explanatory notes.

12. SPONSORING MILITARY ACTIVITY: Enter the name of the departmental project office or laboratory sponsoring *(paying for)* the research and development. Include address.

13. ABSTRACT: Enter an abstract giving a brief and factual summary of the document indicative of the report, even though it may also appear elsewhere in the body of the technical report. If additional space is required, a continuation sheet shall be attached.

It is highly desirable that the abstract of classified reports be unclassified. Each paragraph of the abstract shall end with an indication of the military security classification of the information in the paragraph, represented as *(TS)*, *(S)*, *(C)*, or *(U)*

There is no limitation on the length of the abstract. However, the suggested length is from 150 to 225 words.

14. KEY WORDS: Key words are technically meaningful terms or short phrases that characterize a report and may be used as index entries for cataloging the report. Key words must be selected so that no security classification is required. Identifiers, such as equipment model designation, trade name, military project code name, geographic location, may be used as key words but will be followed by an indication of technical context. The assignment of links, rules, and weights is optional.